Provided for non-commercial research and education use.
Not for reproduction, distribution or commercial use.

This article appeared in a journal published by Elsevier. The attached copy is furnished to the author for internal non-commercial research and education use, including for instruction at the authors institution and sharing with colleagues.

Other uses, including reproduction and distribution, or selling or licensing copies, or posting to personal, institutional or third party websites are prohibited.

In most cases authors are permitted to post their version of the article (e.g. in Word or Tex form) to their personal website or institutional repository. Authors requiring further information regarding Elsevier's archiving and manuscript policies are encouraged to visit:

http://www.elsevier.com/copyright

Author's personal copy

Available online at www.sciencedirect.com
ScienceDirect
Geomorphology 97 (2008) 126–134
GEOMORPHOLOGY
www.elsevier.com/locate/geomorph

Glacial erosion at the fjord onset zone and implications for the organization of ice flow on Baffin Island, Arctic Canada

Jason P. Briner [a,*], Gifford H. Miller [b], Robert Finkel [c], Dale P. Hess [a]

[a] *Geology Department, University at Buffalo, Buffalo, NY 1460, USA*
[b] *Institute of Arctic and Alpine Research, University of Colorado, Boulder, CO 80303, USA*
[c] *Center for Accelerator Mass Spectrometry, Lawrence Livermore National Laboratory, Livermore, CA 94550, USA*

Received 9 September 2006; received in revised form 10 November 2006; accepted 25 February 2007
Available online 23 June 2007

Abstract

Organized conduits of fast ice flow at the fringe of present and past ice sheets move the majority of ice from ice sheet interior to periphery. These relatively narrow corridors play a critical role in feedbacks between landscape evolution and ice sheet dynamics. Here we combine bedrock ^{10}Be concentrations with distribution of lakes on Baffin Island, Arctic Canada, to constrain the pattern of glacial modification at a fjord onset zone — the region of increasing relief from the continental interior to the fjord head. High lake density and a lack of ^{10}Be inheritance in the valley bottom indicate significant glacial scouring for some duration of the last glacial cycle. In contrast, ^{10}Be inheritance and a lack of lakes at higher elevations indicate a lack of glacial scour and only slight glacial modification despite the entire region being covered by the Laurentide Ice Sheet during the last glaciation. This pattern of glacial erosion at the fjord onset zone is similar to what is found in the outer fjords ~100 km toward the last glacial maximum ice margin, and indicates that ice flow becomes organized well inland from the fjorded coast. The relief-generating process of selective linear erosion occurs at the fjord onset zone and was responsible for evolving Baffin Island fjords even in the late Quaternary.
© 2007 Elsevier B.V. All rights reserved.

Keywords: Glacial erosion; Fjord; Cosmogenic radionuclides; Ice sheet

1. Introduction

Narrow corridors of fast ice flow play a critical role in the overall behavior of ice sheets. Fast-flowing outlet glaciers and ice streams move the bulk of ice from ice sheet interior regions to ice sheet peripheries (Bentley, 1987; Bennett, 2003). Likewise, these organized conduits of fast ice flow are the foci of glacial erosion, and therefore of intense landscape modification (Sugden, 1978; Staiger et al., 2005). Nowhere is this glacial impact more dramatic than along fjorded coastlines at the fringe of glaciated continents. However, despite a general understanding of several processes involved in the formation of fjords (e.g., Shoemaker, 1986; Harbor et al., 1988), empirically derived spatial distributions of glacial erosion rates and the patterns of fjord development through the Quaternary ice age are largely non-existent.

Although the highest rates of glacial incision may have occurred early during the Quaternary (e.g., Shuster et al., 2005), recent cosmogenic radionuclide data indicate that fjords are still evolving and relief is still being produced

* Corresponding author. Tel.: +1 716 645 6800.
E-mail addresses: jbriner@buffalo.edu (J.P. Briner), gmiller@colorado.edu (G.H. Miller), finkel1@llnl.gov (R. Finkel), dalehess@buffalo.edu (D.P. Hess).

0169-555X/$ - see front matter © 2007 Elsevier B.V. All rights reserved.
doi:10.1016/j.geomorph.2007.02.039

Author's personal copy

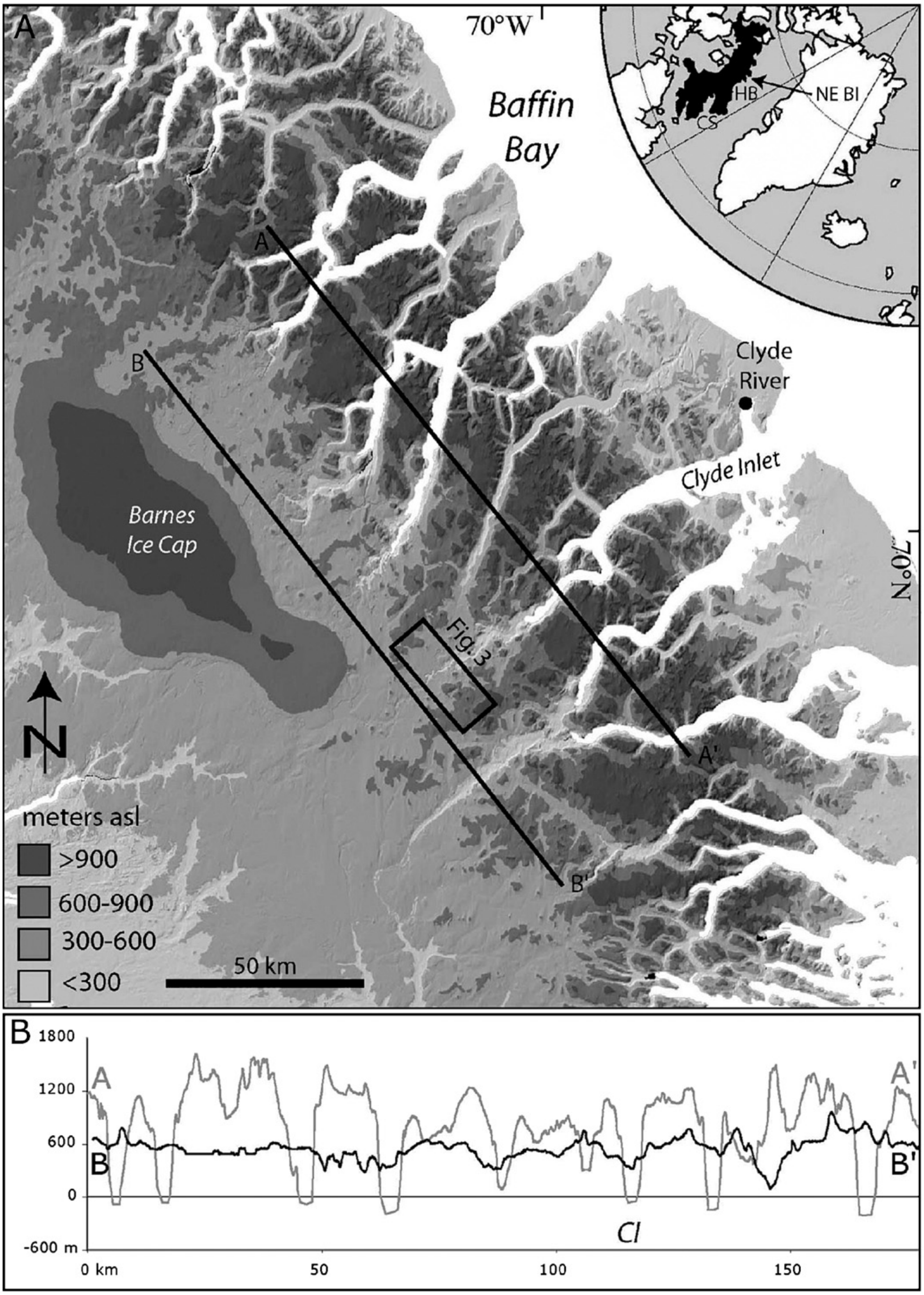

Fig. 1. A. Contoured shaded relief digital elevation map showing topographic setting of the fjord onset region of northeastern Baffin Island (location shown in inset; NE BI = northeastern Baffin Island; HB = Home Bay; CS = Cumberland Sound). B. Transects A–A′ and B–B′ correspond to topographic profiles in lower panel that show increasing entrenchment of valleys and an increase in overall relief that exemplifies "fjord onset" topography. CI = Clyde Inlet.

Author's personal copy

along many high-latitude continental margins (e.g., Staiger et al., 2005; Briner et al., 2006). A variety of applications of cosmogenic radionuclides have constrained ice sheet erosion along ice sheet interiors (Fabel et al., 2002; Stroeven et al., 2002; Li et al., 2005; Harbor et al., 2006; Staiger et al., 2006) and fjords (Briner et al., 2003; Marquette et al., 2004; Staiger et al., 2005). On Baffin Island, regions between the ice sheet interior and periphery have yet to be explored with cosmogenic radionuclides, but are important for understanding how inland ice flow becomes organized to exploit the efficient conduits at fjorded margins.

Here, we focus on the glacial erosion pattern at the fjord onset zone — the region of increasing relief from the continental interior to the fjord head. The fjord onset zone is where fast ice flow initiates. Therefore, understanding basal ice sheet processes in this zone is important for modeling overall ice sheet behavior; in order to model ice sheets properly, empirical data on bed conditions are critical. And, because the rate of glacial erosion is proportional to ice discharge (e.g., Paterson, 1994; Anderson et al., 2006), understanding the pattern of glacial erosion in the fjord onset zone is also important for constraining the pattern and style of fjord landscape evolution. Our goals are to 1) combine apparent ^{10}Be ages and patterns of ice-scoured bedrock to determine the spatial pattern of glacial erosion at a fjord onset zone on north-central Baffin Island (Fig. 1), 2) use these empirical data as constraints in future ice sheet modeling efforts, and 3) eventually elucidate the relationships and feedbacks between ice sheet behavior and fjord landscape evolution.

2. Baffin Island Fjords

The northeastern coast of Baffin Island (Fig. 1) is dissected by dozens of long and deep fjords (up to 120 km long and 800 m below sea level; total relief >2 km; Sugden and John, 1976; Dowdeswell and Andrews, 1985; Syvitski et al., 1987). Glacial erosion has progressed through the coastal mountain range such that the heads of Baffin Island fjords are presently 20 to 30 km *inland* from the range crest. From their heads, fjords typically deepen in steps, are deepest where the range is highest, shallow toward their mouths, and then transition into >200-m-deep troughs that cross the continental shelf (Fig. 1; Løken and Hodgson, 1971). Inland from the fjord heads, valleys become less deep and narrow toward the interior Baffin Island plateau at ~600 m above sea level (m asl). This fjord onset region is characterized by moderate relief with rounded summits between 800 and 1200 m asl.

Our study takes place inland from Clyde Inlet, a 120-km-long fjord that was a major passageway for outlet glaciers and ice streams that drained the northeastern Laurentide Ice Sheet (LIS) during the last glacial maximum (LGM; Briner et al., 2005, 2006). The lowermost portion of the valley that feeds Clyde Inlet holds a rich record of raised marine features (Briner et al., 2007). Farther inland, the landscape is characterized by glacially scoured bedrock at low elevations and mature regolith (blockfield) at high elevations (Fig. 2); in places, moraines separate the two landscape types (Dredge, 2004).

We have recently investigated the glacial history and ice sheet dynamics in the Clyde Inlet region using cosmogenic radionuclides in bedrock and erratic boulders to define the style and extent of Late Quaternary glaciation (Briner et al., 2003, 2005, 2006; Davis et al., 2006; Briner et al., 2007). This work built on extensive field mapping undertaken in the 1960s, when chronological control was dominantly provided by ^{14}C dates on marine shells in raised marine deposits and coastal sediment exposures (e.g., Ives, 1966; Løken, 1966; Miller et al., 1977; Andrews and Ives, 1978). The terrain west of the mountain range crest on eastern Baffin Island was completely inundated by the LIS during the LGM (Briner et al., 2005; 2006), and presumably during earlier Middle and Late Quaternary glaciations. The terrain east of the range crest was also largely overwhelmed by the LIS, which terminated on the continental shelf of Baffin Bay during the LGM (Briner et al., 2005). The exact margin of the LIS along the continental shelf is not yet known.

Cosmogenic radionuclide concentrations in bedrock along vertical profiles across Clyde Inlet indicate that extensive LGM glacial erosion was limited to the primary fjord conduits, and even there, bedrock was only eroded >2 m in the lower ~200 m of the fjords (Briner et al., 2006). Away from the steep fjord confines, weathered bedrock and tor-like forms have apparent cosmogenic exposure ages >60 ka, but erratics resting on them have ages <15 ka, indicating that cold-bedded LGM ice invaded most of the upland regions, but performed little landscape modification (Briner et al., 2006). Collectively, this work points to a model of selective erosion of the fjords by an overriding ice sheet with varying basal thermal (and erosional) regimes that are largely controlled by bed geometry (cf. Sugden, 1978). This work resulted in the need to understand the broader spatial distribution of the selective erosion of fjord landscapes and its impact on landscapes with varying topographic geometry.

3. Methods

Twelve samples for ^{10}Be analysis collected along a cross-valley transect were prepared at the University of Colorado cosmogenic isotope laboratory following

Author's personal copy

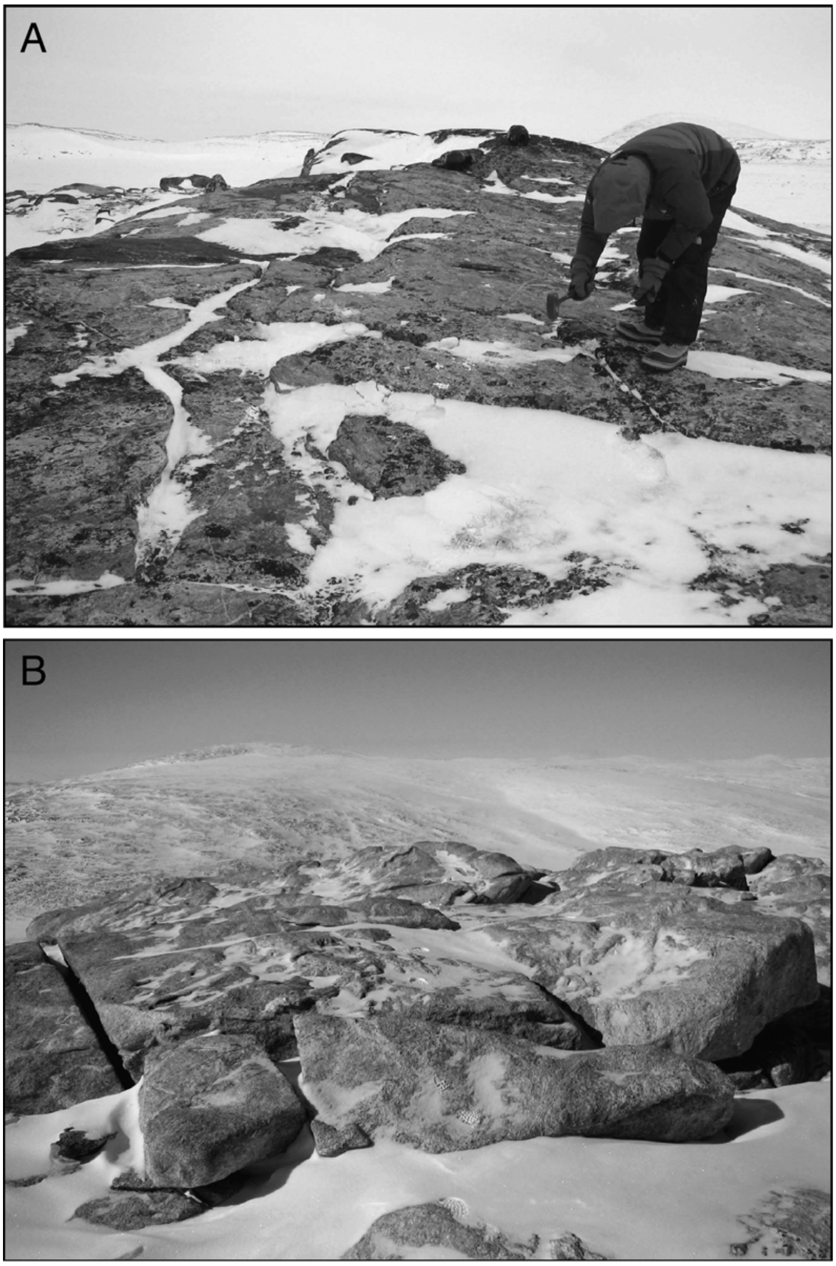

Fig. 2. Photographs of bedrock outcrops typical of warm-bedded erosive ice at low elevations (A) and cold-bedded non-erosive ice at high elevations (B).

procedures modified from Kohl and Nishiizumi (1992). BeO was mixed with Nb metal prior to determination of the $^{10}Be/^{9}Be$ ratios, which were measured by accelerator mass spectrometry at the Center for Accelerator Mass Spectrometry at Lawrence Livermore National Laboratory. Apparent ^{10}Be ages were calculated using a production rate of 5.1 ^{10}Be atoms g^{-1} yr^{-1} (Stone, 2000; Gosse and Stone, 2001). Site-specific production rates were corrected for topographic shielding and sample thickness using standard protocols (e.g., Gosse and Phillips, 2001). Because the samples are from high latitude (~70° N), ^{10}Be production rates are not influenced by time-dependent changes in the geomagnetic field (Gosse and Phillips, 2001). We also consider the effect of elevation change (hence production rate change) resulting from landscape emergence following deglaciation (~70 m for sites ice-free ~9 ka; Briner et al., 2007) for the Holocene portion of sample exposure; the effect is negligible for the valley-bottom samples, and <2% for the upland samples. Ages reported here include only accelerator mass spectrometry measurement uncertainty. We report all ages assuming no significant surface erosion or snow shielding. Rock weathering in the region is negligible (Bierman et al., 1999), and all samples were

Author's personal copy

collected from snow-free sites in May, when snow depths are typically greatest.

As a proxy for ice-scoured bedrock we measured lake density of a study area that encompasses the cosmogenic radionuclide transect (Sugden, 1978; Andrews et al., 1985). Lakes were digitized from a composite image of 1:50,000-scale black and white aerial photos and georeferenced in ArcGIS 9.1. Because our goal is to use lake density as a proxy for glacially scoured bedrock, we removed lakes that are clearly impounded by glacial deposits ($n=12$, 4.8% of the lakes; see Fig. 3). A 1 km square grid was generated in ArcGIS and placed over the study region. Total lake surface area was determined for each 1 km^2 grid cell and overlaid onto

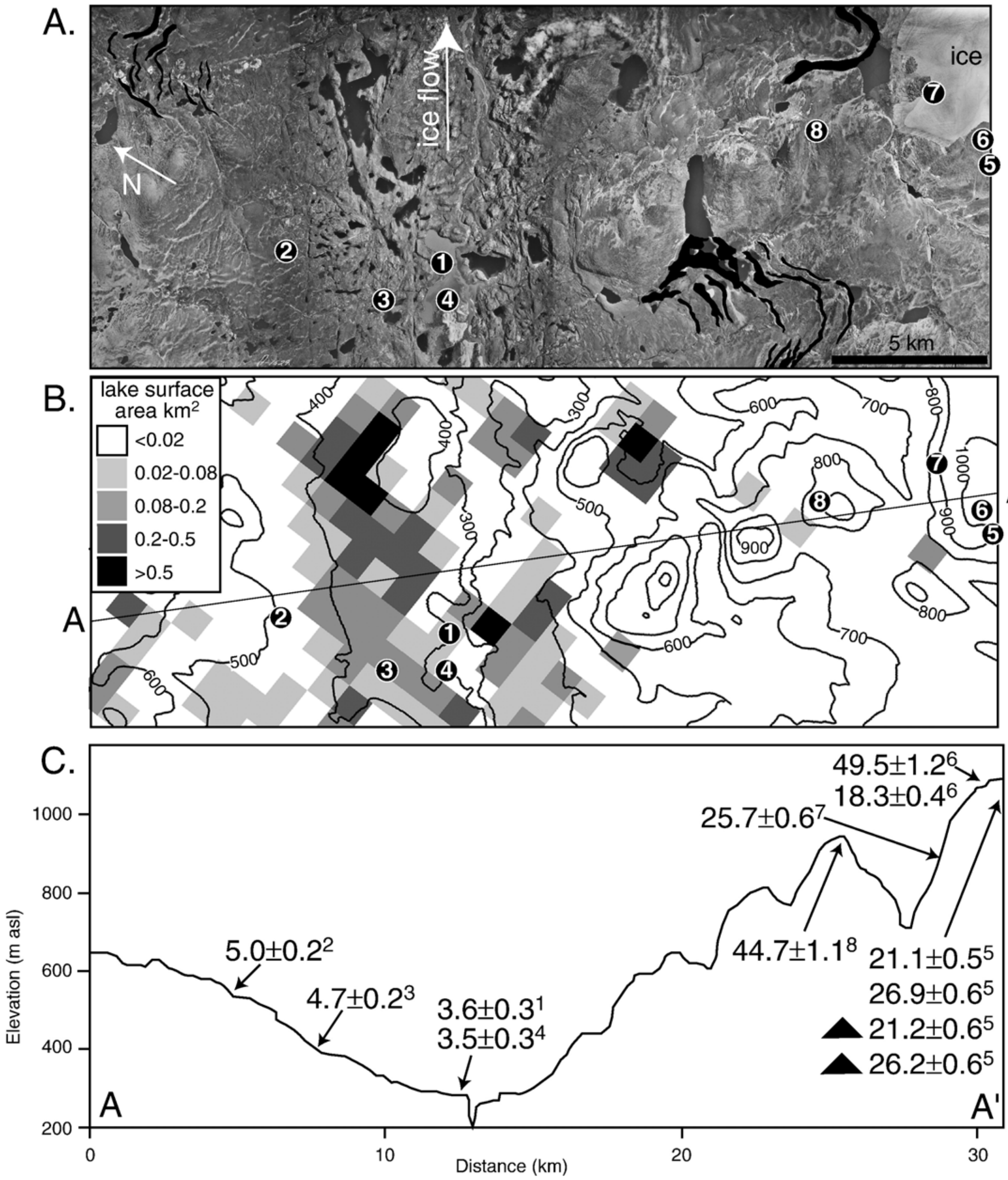

Fig. 3. A. Composite 1:50,000-scale black-and-white aerial photograph image of transect area shown in Fig. 1. Numbers refer to sample sites in Table 1. Generally, ice flowed from the bottom (southwest) to top (northeast). Major moraines are shown to illustrate which lakes are moraine-dammed versus confined within bedrock basins. B. Contoured lake-area density per 1-km^2 grid cells of the transect area showing highest lake-area density below the 500 m contour interval. C. Topographic profile across valley from A–A′ shown in B. Apparent ^{10}Be ages are listed as ka; superscripts refer to sample sites; triangles indicate apparent ^{10}Be ages of erratics.

Author's personal copy

Table 1
Apparent ^{10}Be ages of Clyde Inlet fjord head region

Sample	Latitude (N)	Longitude (W)	Elevation (m asl)	Site # (Fig. 2)	Sample type	Thickness (cm)	$[^{10}Be]$ (10^5 atoms g^{-1})	Apparent ^{10}Be age (ka)
CR04-1	69° 41.679′	71° 10.858′	322	1	Bedrock	1	0.273±0.030	3.5±0.3
CR04-2	69° 41.617′	71° 17.272′	539	2	Bedrock	1.5	0.474±0.044	5.0±0.2
CR04-3	69° 41.651′	71° 14.485′	399	3	Bedrock	3	0.384±0.036	4.7±0.2
CR04-4	69° 41.732′	71° 72.666′	355	4	Bedrock	1.5	0.289±0.035	3.6±0.3
CR04-5	69° 34.566′	70° 44.735′	997	5	Bedrock	1	3.048±0.257	21.1±0.5
CR04-6	69° 34.566′	70° 44.735′	997	5	Bedrock	4	3.784±0.318	26.9±0.6
CR04-7	69° 34.566′	70° 44.735′	997	5	Erratic	5	2.967±0.430	21.2±0.6
CR04-8	69° 34.566′	70° 44.735′	997	5	Erratic	2	3.748±0.316	26.2±0.6
CR04-9	69° 35.674′	70° 47.202′	1157	6	Bedrock	1	3.039±0.778	18.3±0.4
CR04-10	69° 35.661′	70° 47.435′	1161	6	Bedrock	4.5	7.964±0.669	49.5±1.2
CR04-11	69° 36.835′	70° 48.117′	908	7	Bedrock	2	3.405±0.286	25.7±0.6
CR04-12	69° 37.766′	70° 52.825′	939	8	Bedrock	1	6.103±0.513	44.7±1.1

^{10}Be concentrations were measured at Lawrence Livermore National Laboratory and scaled to site-specific altitude using Stone (2000). Apparent ages were calculated assuming zero erosion and sea level, high-latitude production rates of 5.1±0.3 ^{10}Be atoms g^{-1} yr^{-1}. No sample required geometric shield calculations. $^{10}Be/^{9}Be$ isotope ratios were compared to ICN ^{10}Be standards prepared by K. Nishiizumi using a ^{10}Be half-life of 1.5×10^{6} yr.

contoured topography data from 90-m resolution digital elevation data.

4. Results

Apparent ^{10}Be ages were calculated from 10 bedrock samples along a cross-valley transect 20 km inland from the head of Clyde Inlet (Figs. 1 and 3) and ~150 km inland from the LGM ice margin. Four ^{10}Be ages between 3.5±0.3 and 5.0±0.2 ka are from ice-sculpted bedrock in the bottom of the valley between 322 and 539 m asl (Fig. 3; Table 1). Six ^{10}Be ages from frost-riven bedrock slabs on summits between 908 and 1161 m asl range between 18.3±0.5 and 49.5±1.2 ka (Fig. 3; Table 1). In addition, two erratics from a summit at 997 m asl have ^{10}Be ages of 21.2±0.6 and 26.2±0.6 ka. These erratics have noticeably different lithologies and are smaller and more equant shaped than the blockfield slabs, and they are conspicuously perched on top of flat-lying blockfield slabs.

The density of lake area across the study region ranges from 0 to 0.88 km^2 (Fig. 3). Lake-area density is highest between ~250 m asl (the valley bottom) and ~500 m asl; Lakes are virtually absent above ~500 m asl (Fig. 3).

5. Discussion

Bedrock surfaces in the bottom of the Clyde River valley have ^{10}Be ages that are consistent with deglaciation during the middle Holocene. The ^{10}Be ages are significantly younger than the timing of deglaciation at the fjord head ~8 ka (Briner et al., 2007), and depict a thinning lobe of ice that remained along middle Clyde River until it retreated from ~540 m asl at ~5 ka, from ~400 m asl ~4.7 ka, and from the valley floor (320 m asl) by 3.5 ka. These ^{10}Be ages of deglaciation are remarkably close in age to radiocarbon- and lichen-determined ages from Andrews and Barnett (1979), who defined the retreat of the Barnes Ice Cap through the study site ~4700 yr BP. Thus, it appears that sufficient glacial erosion (>2–3 m) occurred during a portion of the last glacial cycle to remove ^{10}Be radionuclides that would have accumulated in bedrock surfaces prior to the last glaciation. This erosion resulted from basal sliding (see ice-sculpted bedrock in Fig. 2), and thus requires warm-bedded conditions at the fjord onset zone of sufficient duration over the last glacial cycle.

Above the valley bottom, somewhere between ~550 and ~900 m asl, the LIS apparently transitioned to dominantly non-sliding conditions throughout the last glacial cycle. Never during the last glacial cycle does it appear that ice slid across these surfaces for any significant period of time due to the lack of polish, striae, or ice-sculpted features (Fig. 2). And, the ^{10}Be concentration in all bedrock samples is higher than would have accumulated since the last deglaciation. Thus, these concentrations require some component of ^{10}Be to have been inherited from prior to the last glaciation. However, the surfaces likely have experienced some form of glacial disturbance (e.g., rotated blocks in a basal shear zone; Atkins et al., 2002) during the last glacial cycle because some samples have concentrations significantly lower than highly weathered tor-like forms on uplands along the outer fjords (Briner et al., 2006). Miller et al. (2006) report companion ^{26}Al data for the two samples reported here with the highest ^{10}Be concentration (CR04-10 and CR04-12); these ^{26}Al concentrations, when combined with the ^{10}Be concentrations, require >450 kyr of surface history. On the

Author's personal copy

other hand, two additional companion ^{26}Al measurements on samples with lower ^{10}Be concentrations (CR04-6 and CR04-9) yield ^{26}Al/^{10}Be ratios that suggest <200 kyr of surface history (Miller et al., 2006). The scatter in apparent ^{10}Be ages (18 to 50 ka) at these high elevations (908 to 1161 m asl), which show no correlation to elevation (Fig. 3; Table 1), may indicate that some sites are more glacially modified than others, although the exact process and timing of this seemingly stochastic modification is unclear.

The two erratic samples have apparent ^{10}Be ages that are similar in age to two blockfield samples from the same summit, and overlap with the age range of all the samples from the upland blockfields. The apparent ^{10}Be ages of the erratics also pre-date deglaciation of the summit (~13 ka based on in-situ ^{14}C exposure ages from summit bedrock; Miller et al., 2006), and thus either were deposited during the last glaciation with inheritance or were emplaced during an earlier glacial episode and subsequently overrun. Either explanation is equally plausible. The erratics could have originated from intermediately weathered terrain similar to the summit upon which they rest. Or, they could have been transported to the summit prior to the last glaciation, and subsequently accumulated ^{10}Be at their present location. Both cases require widespread cold-bedded ice conditions in this region during the late Quaternary. In addition, these results warrant consideration of inheritance when using exposure dating on upland erratics to date deglaciation.

The pattern of highest lake density in the Clyde River valley bottom coincides with the intense glacial scouring revealed by the ^{10}Be data. Lake density in glaciated terrains has long been used as a proxy for glacial scouring; Sugden (1978) calculated the density of lakes per 400 km^2 across the entire footprint of the LIS and found that belts of high lake density coincided with his simulation of LIS scouring (Sugden, 1977). Even at this scale, the lake density pattern revealed intense glacial scouring in several of the major topographic lows on Baffin Island that would have funneled LIS outlets into the adjacent seas (e.g., those that feed Cumberland Sound and Home Bay; Fig. 1). Later, Andrews et al. (1985) used lake density (lakes per 30’ by 30’ gridcells) to examine the pattern of LIS erosion on Baffin Island, focusing on southern and western Baffin Island. A large range in lake density was used to reveal patterns of glacial erosion (Andrews et al., 1985). These results indicate that the density of lakes can reveal the onset of glacial scour along the Baffin Island fjord zone.

These empirical data support the process of selective linear erosion (Sugden, 1978) occurring at the Baffin Island fjord onset zone, ~150 km inland from the LGM margin of the LIS (Briner et al., 2005). This study adds to a growing body of recent literature that supports the selective erosion of ice sheets related to basal thermal conditions, which are in turn dictated by subglacial topography (e.g., Kleman and Stroeven, 1997; Hall and Glasser, 2003; Marquette et al., 2004; Li et al., 2005; Staiger et al., 2005; Sugden et al., 2005; Briner et al., 2006; Phillips et al., 2006). Although the pattern of erosion in the fjord onset zone is similar to that in the outer fjords (Briner et al., 2006), the dimension of the scoured zone is smaller and bedrock weathering at high elevations is less intense than in the outer fjords. The absence of tors and lower amounts of ^{10}Be inheritance in the uplands of the fjord onset region versus on the uplands surrounding the outer fjords implies that there is more glacial modification of inter-valley surfaces in the fjord onset zone. Thus, the rate of relief generation is apparently greater in the outer fjords than the fjord onset zone.

The presence of differential erosion at the fjord onset zone implies that the organization of efficient ice flow conduits along ice sheet peripheries initiates inland of soft sediment-floored fjords where basal sliding is promoted. Thus, sliding conditions and the onset of fast ice flow may occur inland of fjord heads. However, the ^{10}Be inventory at the fjord onset zone reflects the pattern of subglacial erosion integrated over the last glacial cycle. Hence, it is difficult to know if sliding conditions occur in the fjord onset zone during glacial maxima or just during advance and retreat phases. Regardless, this pattern of average differential ice sheet erosion conditions inland of mountain landscapes is likely due to an increase in ice discharge in this region of converging topography (cf. Løken and Hodgson, 1971; Shoemaker, 1986; MacGregor et al., 2000; Anderson et al., 2006). This pattern leads to warm-bedded, sliding (erosive) conditions focused in topographic lows and cold-bedded conditions (non-erosive) at higher elevations. These findings imply that fjords are still evolving along the fringe of the Canadian Shield, and that the fjord onset zone likely plays a key role in feedbacks between topography, ice sheet basal-thermal regime, and glacial erosion.

6. Conclusion

The study of the relationship between ice sheet flow and landscape evolution is benefited by cosmogenic radionuclide techniques. The poorly vegetated, rocky terrain of Baffin Island, with its highly dissected continental margin, is particularly well suited to studying

Author's personal copy

ice sheet–landscape interactions. This study provides empirical field data that reveal the process of selective ice sheet erosion occurring where the LIS first encounters continental edge topography on Baffin Island. The results imply that ice sheet flow is highly dictated by bed topography and begins to organize peripheral conduit flow inland of major topographic obstacles. The convergence of ice into established, but evolving, conduits is likely part of a positive feedback process between trough incision and ice flow, with the partitioning of polythermal ice into warm-bedded (erosive) and cold-bedded (protective) conditions being an important component. The monitoring of subglacial erosion (and hence, former basal thermal conditions) with cosmogenic radionuclides, on Baffin Island and elsewhere, can parameterize bed conditions for numerical ice sheet modeling.

Acknowledgements

We thank Jamesee Qillaq, Jason Hainnu and other friendly people of Clyde River for field logistical support. Field work on Baffin Island was supported by NSF grant OPP- 0138586. Cosmogenic radionuclide measurements were performed under the auspices of the U.S. Department of Energy by the University of California, Lawrence Livermore National Laboratory under contract number W-7405-Eng-48. This manuscript benefited by thoughtful reviews from Clas Hättestrand and Henriette Linge.

References

Anderson, R.S., Molnar, P., Kessler, M.A., 2006. Features of glacial valley profiles simply explained. Journal of Geophysical Research 111, F01004. doi:10.1029/2005JF000344.

Andrews, J.T., Barnett, D.M., 1979. Holocene (Neoglacial) moraine and proglacial lake chronology, Barnes Ice Cap, Canada. Boreas 8, 341–358.

Andrews, J.T., Ives, J.D., 1978. "Cockburn" nomenclature and the late Quaternary history of the eastern Canadian Arctic. Arctic and Alpine Research 20, 617–633.

Andrews, J.T., Clark, P.U., Stravers, J.A., 1985. The pattern of glacial erosion across the eastern Canadian Arctic. In: Andrews, J.T. (Ed.), Quaternary Environments: Eastern Canadian Arctic, Baffin Bay, West Greenland. Allen & Unwin, Winchester, London, pp. 69–92.

Atkins, C.B., Barrett, P.J., Hicock, S.R., 2002. Cold glaciers erode and deposit: evidence from Alan Hills, Antarctica. Geology 30, 659–662.

Bennett, M.R., 2003. Ice streams as the arteries of an ice sheet: their mechanics, stability and significance. Earth-Science Reviews 61, 309–339.

Bentley, C.R., 1987. Antarctic ice streams: a review. Journal of Geophysical Research 92, 8843–8858.

Bierman, P.R., Marsella, K.A., Patterson, C., Davis, P.T., Caffee, M., 1999. Mid-Pleistocene cosmogenic minimum-age limits for pre-Wisconsinan glacial surfaces in southwestern Minnesota and southern Baffin Island: a multiple nuclide approach. Geomorphology 27, 25–39.

Briner, J.P., Miller, G.H., Davis, P.T., Bierman, P.R., Caffee, M., 2003. Last Glacial Maximum ice sheet dynamics in Arctic Canada inferred from young erratics perched on ancient tors. Quaternary Science Reviews 22, 437–444.

Briner, J.P., Miller, G.H., Davis, P.T., Finkel, R., 2005. Cosmogenic exposure dating in Arctic glacial landscapes: implications for the glacial history of northeastern Baffin Island, Canada. Canadian Journal of Earth Sciences 42, 67–84.

Briner, J.P., Miller, G.H., Davis, P.T., Finkel, R.C., 2006. Cosmogenic radionuclides from fiord landscapes support differential erosion by overriding ice sheets. Geological Society of America Bulletin 118, 406–420.

Briner, J.P., Overeem, I., Miller, G.H., Finkel, R.C., 2007. The deglaciation of Clyde Inlet, northeastern Baffin Island, Arctic Canada. Arctic Canada. Journal of Quaternary Science 22, 223–232.

Davis, P.T., Briner, J.P., Coulthard, R.D., Finkel, R.C., Miller, G.H., 2006. Preservation of arctic landscapes overridden by cold-based ice sheets. Quaternary Research 65, 156–163.

Dowdeswell, E.K., Andrews, J.T., 1985. The fiords of Baffin Island: description and classification. In: Andrews, J.T. (Ed.), Quaternary Environments: Eastern Canadian Arctic, Baffin Bay, West Greenland. Allen & Unwin, Winchester, London, pp. 93–123.

Dredge, L.A., 2004. Surficial geology, McBeth Fiord (west half), central Baffin Island, Nunavut. Geological Survey of Canada, Map 2074A, scale 1:250,000.

Fabel, D., Stroeven, A.P., Harbor, J., Kleman, J., Elmore, D., Fink, D., 2002. Landscape preservation under Fennoscandian ice sheets determined from in situ produced ^{10}Be and ^{26}Al. Earth and Planetary Science Letters 201, 397–406.

Gosse, J.C., Phillips, F.M., 2001. Terrestrial in situ cosmogenic nuclides: theory and application. Quaternary Science Reviews 20, 1475–1560.

Gosse, J.C., Stone, J.O., 2001. Terrestrial cosmogenic nuclide methods passing milestones toward paleo-altimetry. Eos, Transactions of the American Geophysical Union. 82, 82, 86, 89.

Hall, A.M., Glasser, N.F., 2003. Reconstructing the basal thermal regime of an ice stream in a landscape of selective linear erosion: Glen Avon, Cairngorm Mountains, Scotland. Boreas 32, 191–207.

Harbor, J.M., Hallet, B., Raymond, C.F., 1988. A numerical-model of landform development by glacial erosion. Nature 333, 347–349.

Harbor, J., Stroeven, A.P., Fabel, D., Clarhäll, A., Kleman, J., Li, Y., Elmore, D., Fink, D., 2006. Cosmogenic nuclide evidence for minimal erosion across two subglacial sliding boundaries of the late glacial Fennoscandian ice sheet. Geomorphology 75, 90–99.

Ives, J.D., 1966. Block fields, associated weathering forms on mountain tops and the Nunatak Hypothesis. Geografiska Annaler 48A, 220–223.

Kleman, J., Stroeven, A.P., 1997. Preglacial surface remnants and Quaternary glacial regimes in northwestern Sweden. Geomorphology 19, 35–54.

Kohl, C.P., Nishiizumi, K., 1992. Chemical isolation of quartz for measurement of in-situ-produced cosmogenic nuclides. Geochimica et Cosmochimica Acta 56, 3583–3587.

Li, Y., Harbor, J., Stroeven, A.P., Fabel, D., Kleman, J., Fink, D., Caffee, M., Elmore, D., 2005. Ice sheet erosion patterns in valley systems in northern Sweden investigated using cosmogenic nuclides. Earth Surface Processes and Landforms 30, 1039–1049.

Løken, O.H., 1966. Baffin Island refugia older than 54,000 years. Science 153, 1378–1380.

Author's personal copy

Løken, O.H., Hodgson, D.A., 1971. On the submarine geomorphology along the east coast of Baffin Island. Canadian Journal of Earth Sciences 8, 185–195.

MacGregor, K.C., Anderson, R.S., Anderson, S.P., Waddington, E.D., 2000. Numerical simulations of glacial-valley longitudinal profile evolution. Geology 28, 1031–1034.

Marquette, G.C., Gray, J.T., Gosse, J.C., Courchesne, F., Stockli, L., Macpherson, G., Finkel, R., 2004. Felsenmeer persistence under non-erosive ice in the Torngat and Kaumajet mountains, Quebec and Labrador, as determined by soil weathering and cosmogenic nuclide exposure dating. Canadian Journal of Earth Sciences 41, 19–38.

Miller, G.H., Andrews, J.T., Short, S.K., 1977. The last interglacial-glacial cycle, Clyde foreland, Baffin Island, N.W.T.: stratigraphy, biostratigraphy, chronology. Canadian Journal of Earth Sciences 14, 2824–2857.

Miller, G.H., Briner, J.P., Lifton, N.A., Finkel, R.C., 2006. Limited ice-sheet erosion and complex exposure histories derived from in situ cosmogenic ^{10}Be, ^{26}Al and ^{14}C on Baffin Island, Arctic Canada. Quaternary Geochronology 1, 74–85.

Paterson, W.S.B., 1994. The Physics of Glaciers, 3rd ed. Pergamon Press, Oxford.

Phillips, W.M., Hall, A.M., Mottram, R., Fifield, K.L., Sugden, D.E., 2006. Cosmogenic ^{10}Be and ^{26}Al exposure ages of tors and erratics, Cairngorm Mountains, Scotland: timescales for the development of a classic landscape of selective linear glacial erosion. Geomorphology 73, 222–245.

Shoemaker, E.M., 1986. The formation of fjord thresholds. Journal of Glaciology 32, 65–71.

Shuster, D.L., Ehlers, T.A., Rusmore, M.E., Farley, K.A., 2005. Rapid glacial erosion at 1.8 Ma revealed by ^{4}He/^{3}He thermochronometry. Science 310, 1668–1670.

Staiger, J.K.W., Gosse, J.C., Johnson, J.V., Fastook, J., Gray, J.T., Stockli, D.F., Stockli, L., Finkel, R., 2005. Quaternary relief generation by polythermal glacier ice. Earth Surface Processes and Landforms 30, 1145–1159.

Staiger, J.W., Gosse, J.C., Little, E.C., Utting, D.J., Finkel, R., Johnson, J.V., Fastook, J., 2006. Glacial erosion and sediment dispersion from detrital cosmogenic nuclide analysis of till. Quaternary Geochronology 1, 29–42.

Stone, J.O., 2000. Air pressure and cosmogenic isotope production. Journal of Geophysical Research, [Solid Earth] 105, 23753–23759.

Stroeven, A.P., Fabel, D., Harbor, J., Hättestrand, C., Kleman, J., 2002. Quantifying the erosional impact of the Fennoscandian ice sheet in the Tornetrask-Narvik corridor, northern Sweden, based on cosmogenic radionuclide data. Geografiska Annaler 84A, 275–287.

Sugden, D.E., 1977. Reconstruction of morphology, dynamics, thermal characteristics of Laurentide Ice Sheet at its maximum. Arctic and Alpine Research 9, 21–47.

Sugden, D.E., 1978. Glacial erosion by the Laurentide Ice Sheet. Journal of Glaciology 83, 367–391.

Sugden, D.E., John, B.S., 1976. Glaciers and Landscape. Arnold, London, p. 376.

Sugden, D.E., Balco, G., Cowdery, S.G., Stone, J.O., Sass III, L.C., 2005. Selective glacial erosion and weathering zones in the coastal mountains of Marie Byrd Land, Antarctica. Geomorphology 67, 317–334.

Syvitski, J.P.M., Burrell, D.C., Skei, J.M., 1987. Fjords: Processes and Products. Springer, New York, p. 379.